Theory of antiferroelectric phase transitions

Pierre Tolédano[1] and Mael Guennou[2,*]

[1]*Laboratoire de Physique des Systèmes Complexes, Université de Picardie, 80000 Amiens, France*

[2]*Materials Research and Technology Department, Luxembourg Institute of Science and Technology, 41 rue du Brill, L-4422 Belvaux, Luxembourg*

(Received 20 January 2016; revised manuscript received 6 May 2016; published 11 July 2016)

At variance with structural ferroic phase transitions which give rise to macroscopic tensors coupled to macroscopic fields, criteria defining antiferroelectric (AFE) phase transitions are still under discussion due to the absence of specific symmetry properties characterizing their existence. They are recognized by the proximity of a ferroelectric (FE) phase induced under applied electric field, with a double hysteresis loop relating the induced polarization to the electric field and a typical anomaly of the dielectric permittivity. Here, we show that there exist indeed symmetry criteria defining AFE transitions. They relate the local symmetry of the polar crystallographic sites emerging at an AFE phase transition with the macroscopic symmetry of the AFE phase. The dielectric properties of AFE transitions are deduced from a Landau theoretical model in which ferroelectric and ferrielectric phases are shown to stabilize as the result of specific symmetry-allowed couplings of the AFE order parameter with the field-induced polarization.

DOI: 10.1103/PhysRevB.94.014107

I. INTRODUCTION

The relation between antiferroelectricity and ferroelectricity is traditionally assumed to be analogous to the relation between antiferromagnetism and ferromagnetism. However, there is an essential difference between the symmetry properties governing spin and dipole orderings. In the paramagnetic state, time-reversal symmetry, which is not a symmetry operation in real space, exists everywhere and is lost at the transition to the antiferromagnetic or ferromagnetic states, only surviving in combination with part of the symmetry operations associated with the crystallographic space group of the atomic structure [1]. By contrast, in the paraelectric (PA) phase the symmetry operations of the crystal space group are localized in space. As such, a paraelectric "state" does not exist by itself in the same sense as the paramagnetic state, and all crystal structures displaying nonpolar symmetries can be potentially antiferroelectric.

Definitions of antiferroelectricity involve the microscopic picture of antiparallel dipoles, the existence of an electric field induced FE phase associated with a double hysteresis loop relating the electric polarization and the field, and a characteristic anomaly of the dielectric permittivity [2–4]. A symmetry-based definition of AFE transitions is still lacking, in spite of previous attempts [5,6] inspired from a displacive picture, and focused on a definition for atomic displacement patterns associated to an AFE "soft-mode" as the driving mechanism of the PA to AFE transition. Such a definition is not well suited for describing the many important cases of order-disorder antiferroelectrics that represent a majority of the well-established AFE transitions. Besides, they are not linked to specific physical properties, so that the definition is of little use. This led some authors to state that antiferroelectricity was an ill-defined and hardly useful notion [7].

In this work we propose a definition of AFE transitions which stems from definite symmetry conditions fulfilled exclusively in AFE materials (Sec. II). The dielectric properties characterizing AFE transitions are deduced from a Landau model in which ferroelectric (FE) and ferrielectric (FI) phases are shown to stabilize under specific field-induced couplings of the AFE order parameter with the electric polarization (Sec. III). In Sec. IV, the traditional analogy between antiferroelectricity and antiferromagnetism, the concept of local polarization assumed in our theoretical description, and the nature of the AFE order parameter are discussed. Last, in Sec. V our results are summarized and the difference of our theoretical approach with Kittel's model of antiferroelectricity [8] is underlined.

II. SYMMETRY-BASED DEFINITION OF AFE TRANSITIONS

PA–AFE transitions are structural transitions between phases displaying nonpolar space groups, which exhibit under applied electric field a typical dielectric behavior. A Landau symmetry analysis of the order parameters associated with the PA–AFE transitions reported experimentally shows that the transitions occur exclusively in materials which do not have a stable FE phase in their phase diagram at zero fields. It indicates that their dielectric properties are purely field-induced effects. Since only a limited number of structural phase transitions between nonpolar space groups exhibit such dielectric properties, PA–AFE transitions should obey restrictive and specific conditions. These conditions have so far not been found from the macroscopic symmetries of the PA or AFE phases alone. The specificity of PA–AFE transitions has therefore to be searched in the microscopic features of their transition mechanism. Here we show that two symmetry-based conditions have to be fulfilled for a phase transition to qualify as PA–AFE. A first condition deals with the local changes occurring at the transition.

Condition 1. At the PA–AFE transition, a set of crystallographic sites undergo a symmetry lowering that results in the emergence of polar sites and gives rise to a local polarization.

*mael.guennou@list.lu

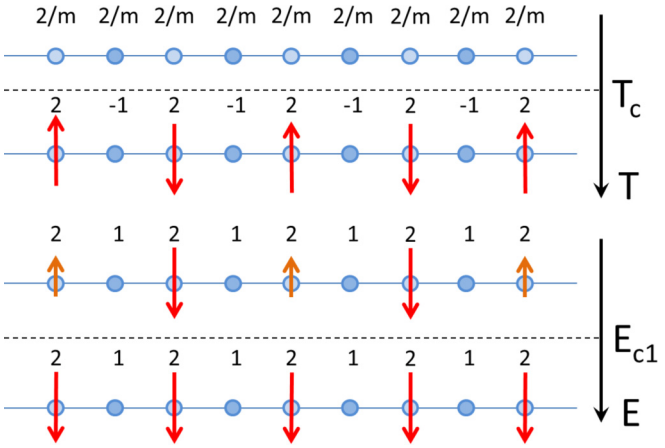

FIG. 1. Illustration of the local symmetry-breaking mechanism corresponding to Condition 1. In the PA phase, all sites of an atomic row have a nonpolar site symmetry $2/m$. At the AFE transition at T_c the symmetry of every other atomic site lowers to 2. The sites located at mid distance preserve their inversion center yielding the onset of antiparallel dipoles on the polar sites. An electric field oriented along the dipoles favors a ferrielectric configuration. Above a coercive field E_{c1} a FE dipolar order arises.

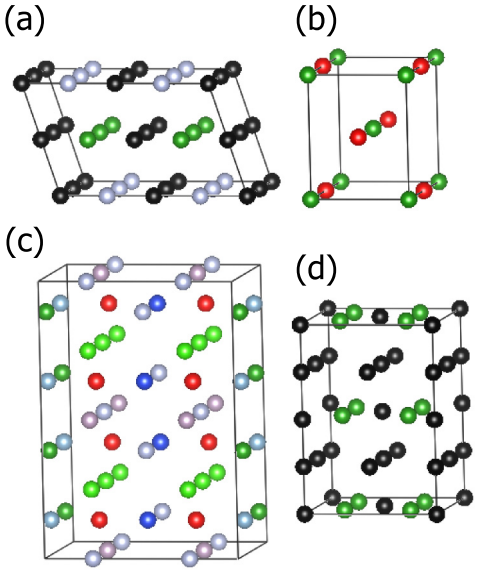

FIG. 2. Emerging polar sites at the AFE transitions in (a) $Cu(HCOO)_2 \cdot 4H_2O$ [30], (b) KCN [10], (c) $PbZrO_3$ [11], and (d) at the non-AFE transition in $SrTiO_3$. Colored spheres indicate the polar sites carrying antiparallel dipoles in the AFE phase, whereby crystallographically equivalent sites are drawn in the same color. At sites drawn in black, no local polarization can emerge.

Figure 1 illustrates the local symmetry-breaking mechanism corresponding to condition 1 for a one-dimensional toy model. In the PA phase, all sites have the nonpolar site symmetry $2/m$. At the PA–AFE transition, every other site acquires the polar site symmetry 2 while the sites located in between keep their inversion center, which results in the onset of antiparallel local polarizations on the "active" polar sites, and a nonpolar macroscopic symmetry. The principle is the same in real systems. Figures 2(a)–2(c) show the onset of polar sites in the well-established examples of PA–AFE transitions reported in $Cu(HCOO)_2.4H_2O$ [9], KCN [10], and $PbZrO_3$ [11]. They involve two or four sets of independent polar sites arising from nonpolar sites at the transitions, which may carry antiparallel arrays of dipoles.

The emergence of polar sites and local polarization at PA–AFE transitions constitutes a necessary condition for their existence, but the following additional condition is required for preserving the site symmetries at the macroscopic level, permitting a subsequent stabilization of a FE phase under applied electric field.

Condition 2. The AFE space group has a symmorphic polar subgroup coinciding with the local symmetry of emerging polar sites.

This condition derives from the property that only symmetry operations of the AFE space group forming a symmorphic group preserve the local site symmetries, while screw axes and glide planes modify the symmetry of the local sites. That the emergence of polar sites (condition 1) is not a sufficient condition for the existence of a PA–AFE transition can be exemplified by the ferroelastic transition in $SrTiO_3$, where the dielectric properties characterizing AFE materials have not been detected. Figure 2(d) shows the onset of polar sites of symmetry $mm2$ at its cubic $Pm\bar{3}m$ to tetragonal $I4/mcm$ transition. The symmorphic polar subgroups of $I4/mcm$ are $I4$, $C2$, Cm, and $P1$, the point groups of which differ from $mm2$. Therefore, condition 2 is not fulfilled and the transition in $SrTiO_3$ does not have an AFE character, in spite of the arguable existence of a local polarization on the $mm2$ sites of its tetragonal phase.

Figure 1 shows the local effect of an applied electric field on the emerging polar sites: low fields oriented along the preexisting local polarization favor a ferrielectric (FI) configuration, and above a coercitive E_c field a FE dipolar order arises. The preservation of the polar site symmetry and local polarization by a symmorphic subgroup of the AFE space group allows realizing at the macroscopic level a similar sequence of FI and FE phases induced from the AFE phase under suitably oriented fields. The space group of the FE phase coincides with the symmetry of the PA phase under applied field; it may contain screw axes or glide planes and is always of higher symmetry than the symmorphic subgroup of the AFE phase. Depending on the orientation of the field, the FE phase may involve symmetry operations which do not belong to the AFE space group. The space group of the FI phase is a common polar subgroup of the AFE and FE space groups; it may also have a higher symmetry than the symmorphic space group.

A verification of Conditions 1 and 2 for confirmed AFE materials is summarized in Table I. It shows that the two conditions are unambiguously verified for the corresponding PA–AFE transitions, the highest polar site symmetry coinciding with the maximal symmorphic polar subgroup of the AFE space group. The table indicates the orientation of the electric fields stabilizing a FE phase. Also listed are a number of materials ($BiVO_4$, TeO_2, NdP_5O_{14}) which undergo transitions fulfilling conditions 1 and 2 but have not yet been recognized as antiferroelectric. It contains as well examples of transitions that do not verify condition 1 (NH_4Cl) or condition 2 ($SrTiO_3$). For some of the listed materials ($DyVO_4$, TeO_2,

TABLE I. Verification of conditions 1 and 2 for selected structural transitions in AFE and other materials listed in column (a). Other columns have the following meaning. (b) Space-group changes occurring at the transitions. (c) Crystallographic sites undergoing a lowering of their local symmetry to a polar point group. (d) Symmorphic polar subgroups of the low-symmetry phase space groups coinciding with the emerging polar site symmetries. (e) Couplings between the AFE transition order parameter and the polarization allowing emergence of a field-induced polar phase. (f) Corresponding orientation(s) of the electric field. (g) Space group of the FE phase. In (e) and (f) except for $CsH_3(SeO_3)_2$ only couplings corresponding to nongeneral directions of P and E are given. In (e), η_1 and η_2 are two components of the same transition order parameter except for $PbZrO_3$ where they correspond to different order parameters.

(a)	(b)	(c)	(d)	(e)	(f)	(g)
$CsH_3(SeO_3)_2$	$P\bar{1} \rightarrow P\bar{1}$	$1a : \bar{1} \rightarrow 1$	$P1$	$\eta^2 P^2$	E	$P1$
$Cu(HCOO)_2.4H_2O$	$P2_1/a \rightarrow P2_1/a$	$2a,2b,2c,2d : \bar{1} \rightarrow 1$	$P1$	$\eta^2 P_z^2$	E_z	$P2_1$
KCN	$Immm \rightarrow Pmmn$	$2a,2c : mmm \rightarrow mm2$	$Pmm2$	$\eta^2 P_z^2$	E_z	$Imm2$
$C_4O_4H_2$	$I4/m \rightarrow P2_1/m$	$2a,2b : 4/m \rightarrow m$	$Pm,P1$	$(\eta_1\eta_2,\eta_1^2-\eta_2^2)$	E_{xy}	Cm
		$4c : 2/m \rightarrow m$		$\times(P_xP_y,P_x^2-P_y^2)$,		
		$4d : \bar{4} \rightarrow 1$		$(\eta_1^2+\eta_2^2)P_z^2$	E_z	$I4$
$NH_4H_2PO_4$	$I\bar{4}2d \rightarrow P2_12_12_1$	$4a,4b : \bar{4} \rightarrow 1$	$P1$	idem	E_{xy},E_z	$Cc,Fdd2$
$DyVO_4$	$I4_1/amd \rightarrow Imma$	$4a,4b : \bar{4}m2 \rightarrow mm2$	$Imm2,P1$	$\eta^2 P_z^2$	E_z	$I4_1md$
		$16h : 2_{xy} \rightarrow 1$		$\eta(P_x^2-P_y^2)$	E_{xy}	$Imm2$
$BiVO_4$	$I4_1/a \rightarrow B2/b$	$4a,4b : \bar{4} \rightarrow 2$	$C2$	$\eta^2 P_z^2$	E_z	$I4_1$
				$\eta(P_xP_y,P_x^2-P_y^2)$	E_{xy}	Cc
TeO_2	$P4_12_12 \rightarrow P2_12_12_1$	$4a : 2 \rightarrow 1$	$P1$	$\eta^2 P_z^2$	E_z	$P4_1$
		$8b : 1 \rightarrow 1$		$\eta(P_x^2-P_y^2)$	E_{xy}	$C2$
$PbZrO_3$	$Pm\bar{3}m \rightarrow Pbam$	$3d : 4/mmm \rightarrow m,2$	$Pm,P2$	$(\eta_1^2,\eta_2^2)P_{x,y,z}^2$	$E_{x,y,z}$	$P4mm$
		$1a,1b : m\bar{3}m \rightarrow m,1$	$P1$	$(\eta_1^2,\eta_2^2)P_{xy,yz,zx}^2$	$E_{xy,yz,zx}$	$Amm2$
NdP_5O_{14}	$Pmna \rightarrow P2_1/b$	$4e,4f : 2 \rightarrow 1$	$P1$	ηP_xP_y	E_{xy}	$Pnc2$
		$4h : m \rightarrow 1$		$\eta^2 P_z^2$	E_z	$Pmn2_1$
NH_4Cl	$Pm\bar{3}m \rightarrow P\bar{4}3m$	none				
$SrTiO_3$	$Pm\bar{3}m \rightarrow I4/mcm$	$3d : 4/mmm \rightarrow mm2$	$I4,C2,Cm,P1$	none		

NdP_5O_{14}), the local polarization emerging at the transition results from a symmetry lowering on sites with an already polar site symmetry in the PA phase, which illustrates the property that PA and AFE "states" do not exist *per se* but can only be defined in the context of a PA–AFE phase transition.

As will become apparent in the following, a variety of situations have to be taken into account in real systems. For instance, due to the high energy barrier that may exist between the FI and FE phases, the latter may not always be stabilized at high fields (Sec. IV). Moreover, for specific couplings of the PA–AFE transition order parameter with the polarization, the FE phase becomes unstable, the field-induced FI-FE sequence of phases being replaced by a sequence of two isostructural FI phases (Sec. III). Accordingly, the emergence of a FE phase is not a prerequisite for PA–AFE transitions, and the realization of a double hysteresis loop under high fields can be effective or latent. Therefore, our theoretical analysis allows proposing the following symmetry-based definition which encompasses the variety of experimental situations: PA–AFE transitions are structural transitions between nonpolar phases where the symmetry of crystallographic polar sites emerging at the local scale coincides with the symmetry of a polar symmorphic subgroup of the AFE space group, allowing the emergence of an electric field induced polar phase at the macroscopic scale.

III. DIELECTRIC PROPERTIES OF AFE TRANSITIONS

Application of an electric field E to a nonpolar AFE phase induces a coupling between the AFE order parameter, here labeled η, and the polarization P. The lowest degree coupling between η and P determines the stability and symmetry of a field-induced FE phase, and the orientation of the electric dipoles in the AFE phase. It also establishes the link with the dielectric anomalies typifying AFE transitions. Only couplings of the η^2P^2 or ηP^n $(n \geqslant 2)$ types can be associated with an AFE transition, since only such couplings reflect the remarkable property of AFE transitions to occur in materials which do not have a stable polar phase at zero fields. For a biquadratic η^2P^2 coupling, the dielectric properties of AFE transitions derive from the Landau potential:

$$\phi(\eta,P,T) = \phi_0(T) + \frac{\alpha}{2}\eta^2 + \frac{\beta}{4}\eta^4 + \frac{\gamma}{6}\eta^6 + \frac{P^2}{2\chi_0} + \frac{\delta}{2}\eta^2P^2 - EP, \quad (1)$$

where $\alpha = a(T - Tc)$, and the other phenomenological coefficients are constant. This order-parameter expansion differs from the seminal model by Kittel [8] as it involves a single symmetry-breaking AFE order parameter η, the polarization P being a field-induced order parameter. It expresses the property that a polar phase requires the mediation of the AFE order parameter to be stabilized upon application of an electric field.

Minimizing ϕ with respect to η and P yields the equations of state:

$$\eta(\alpha + \beta\eta^2 + \gamma\eta^4 + \delta P^2) = 0, \quad (2)$$

$$P(1 + \delta\chi_0\eta^2) = \chi_0 E. \quad (3)$$

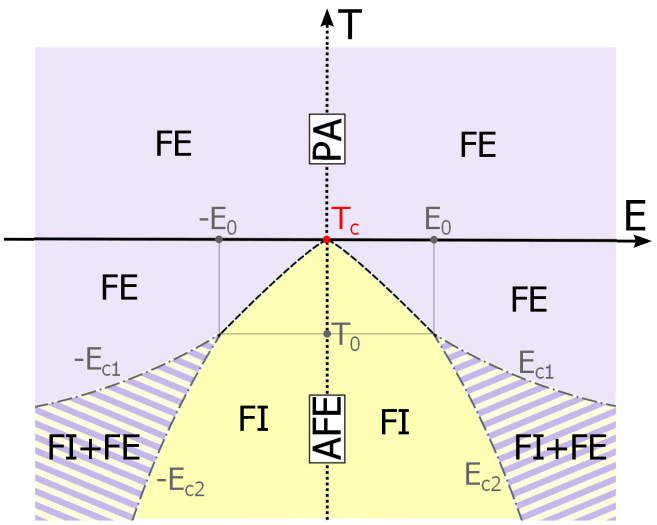

FIG. 3. Theoretical temperature-electric field (T-E) phase diagram associated with the free energy given by Eq. (1) for $\beta > 0$ and $\delta > 0$. Hatched and hatched-dotted curves represent, respectively, second-order transition and limit of stability curves. The thermodynamic paths for $T > T_c$, $T_c > T > T_0$, and $T < T_0$ are described in the text.

At $E = 0$, Eqs. (2) and (3) yield two possible stable phases: the PA phase ($\eta = 0$, $P = 0$) and the AFE phase ($\eta \neq 0$, $P = 0$). For $E \neq 0$ two phases are stabilized: a FE phase ($\eta = 0$, $P \neq 0$) in which the AFE antiparallel dipole configuration is absent, and a phase in which the AFE ordering ($\eta \neq 0$) has a nonzero total polarization ($P \neq 0$), i.e., having either a ferrielectric (FI) dipolar order or a "weak" ferroelectric (WF) order with a canting between antiparallel arrays of dipoles.

Figure 3 shows the location of the PA, AFE, and field-induced FE and FI or WF phases in a theoretical temperature-field T–E phase diagram. For $T \geqslant T_c$ the PA phase ($\eta = 0$, $P = 0$) stable at $E = 0$ transforms into the FE phase ($\eta = 0$, $P = \chi_0 E$) for $E \neq 0$. For $T_c > T > T_0$ the AFE phase [$\eta = \pm(-\frac{-\alpha}{\beta})^{1/2}, P = 0$] stable at $E = 0$ transforms into a FI (or WF) phase for $E \neq 0$, in which the equilibrium values of η and P are given by $\eta = \pm[(-\alpha - \delta P^2)/\beta]^{1/2}$, where P is a real root of the Cardan equation

$$\frac{\delta^2}{\beta} P^3 - \left(\frac{1}{\chi_0} - \frac{\alpha\delta}{\beta}\right) P + E = 0. \tag{4}$$

With increasing field the FI phase transforms across the second-order transition curve

$$E = \pm \frac{1}{\chi_0}\left(-\frac{\alpha}{\delta}\right)^{1/2} \tag{5}$$

into the FE phase, which implies that the FI space group is a subgroup of the FE space group. For $T < T_0$ the transformation of the FI into the FE phase becomes first order, crossing the region of coexistence of the FI and FE phase. With increasing field the FI phase transforms discontinuously into the FE phase, the limit of stability of the FI phase corresponding to the curve E_{c1}, the equation of which is given by the condition $\partial^2_{\eta\eta}\Phi \cdot \partial^2_{PP}\Phi - [\partial^2_{\eta P}\Phi]^2 = 0$ with ($\eta \neq 0$, $P \neq 0$)

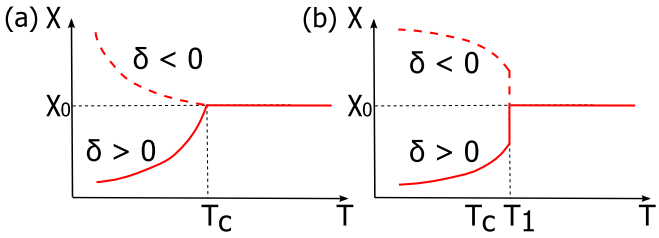

FIG. 4. Temperature dependence of the dielectric susceptibility $\chi(T)$ given by Eq. (4) across a second-order (a) and first-order (b) transition.

corresponding to

$$\frac{3\delta^3}{\beta} P^4 + \delta P^2 \left(\frac{4\delta\alpha}{\beta} - \frac{1}{\chi_0}\right) + \alpha\left(\frac{\delta\alpha}{\beta} - \frac{1}{\chi_0}\right) = 0. \tag{6}$$

The $E_{c1}(T)$ curve is obtained by introducing a real root of Eq. (4) into Eq. (6). With decreasing field the FE phase reaches its limit of stability on the E_{c2} curve corresponding to Eq. (5). The merging point of the E_{c1} and E_{c2} curves provides the values of T_0 and E_0. The first-order transition curve between the FI and FE phases, not shown in Fig. 3, is located between the E_{c1} and E_{c2} curves below T_0. Its equation is given by $\Phi(P_{\rm FI}, \eta_{\rm FI}) = \Phi(P_{\rm FE}, 0)$, where $P_{\rm FE} = \chi_0 E$, $P_{\rm FI}$ is a real root of Eq. (4), and $\eta_{\rm FI} = \pm[(-\alpha - \delta P^2_{\rm FI})/\beta]^{1/2}$.

One can deduce from Eq. (3) the temperature dependence of the dielectric susceptibility at the PA–AFE transition. For a second-order transition ($\beta > 0$) one gets below T_c

$$\chi(T) = \frac{\chi_0}{1 + \delta a \chi_0 \frac{(T_c - T)}{\beta}}, \tag{7}$$

the temperature dependence of which depends on the sign of δ [Fig. 4(a)]. Figure 4(b) shows $\chi(T)$ for a first-order transition ($\beta < 0$) occurring at $T_1 > T_c$, which involves an upward ($\delta < 0$) or downward ($\delta > 0$) discontinuity. AFE transitions verifiy the preceding temperature dependences of $\chi(T)$ for $\delta > 0$, with a downward discontinuity at T_1 for $CsH_3(SeO_3)_2$ [12], $Cu(HCOO)_2 \cdot 4H_2O$ [9], KCN [13,14], $NH_4H_2PO_4$ [15], and $PbZrO_3$ [16] and a decrease below T_c for $C_4O_4H_2$ [17].

Equation (4) provides the electric field dependence $P(E)$ of the polarization. It corresponds to a double hysteresis loop which, as shown in Fig. 3, can be observed for a second-order AFE transition below a temperature $T_0 < T_c$ [Figs. 5(a)–5(d)], whereas for a first-order AFE transition it is observed below $T_1 > T_c$ [Figs. 5(e) and 5(f)]. Characteristic double AFE loops have been observed in a number of AFE transitions, e.g., in $CsH_3(SeO_3)_2$ [12], $Cu(HCOO)_2 \cdot 4H_2O$ [9], or $PbZrO_3$ [16]. Double hysteresis loops are also reported at first-order FE transitions, as for example in $BaTiO_3$ [18]. However, at variance with AFE transitions the two loops are observed within the region of stability of the PA phase and merge into a single loop at the transition to the FE phase.

A biquadratic $\delta\eta^2 P^2$ coupling always exists at AFE transitions. However, a $\mu\eta P^n$ ($n \geqslant 2$) coupling can also be permitted by symmetry, which modifies the previous results.

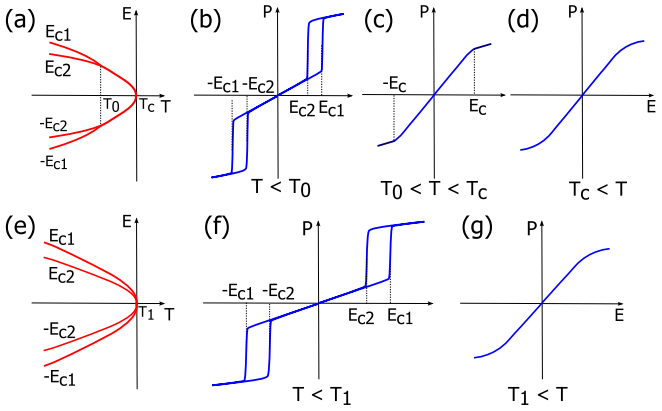

FIG. 5. $E(P)$ and $E_c(T)$ curves deduced from Eqs. (2) and (3) for a second-order PA–AFE transition (a)–(d) and a first-order transition (e)–(g). At low fields the linear behavior of $P(E)$ indicates a progressive transformation of the AFE phase into a FI or WF dipolar order. At a coercive field E_{c1} a discontinuous transition occurs to a FE phase. Reversing the field, $P(E)$ decreases along a different path below a coercive field $E_{c2} < E_{c1}$ forming a loop before reaching the linear regime.

The corresponding equations of state

$$\eta(\alpha + \beta\eta^2 + \gamma\eta^4 + \delta P^2) + \mu P^n = 0, \tag{8}$$

$$P\left(\frac{1}{\chi_0} + \delta\eta^2 + n\mu\eta P^{n-2} + \nu P^2\right) = E \tag{9}$$

do not allow a stable FE phase under applied field but only FI or WF ($\eta \neq 0$, $P \neq 0$) phases, the stabilization of which requires taking into account an additional $\frac{\nu}{4}P^4$ invariant in Φ. A double hysteresis loop can occur at a first-order field-induced phase transition between two isostructural FI or WF phases having different regions of stability. The temperature dependence of the dielectric susceptibility $\chi(T)$ has a similar shape than for a $\delta\eta^2 P^2$ coupling.

ηP^2 couplings exist exclusively for "proper" ferroelastic transitions [19], where η has the symmetry of a spontaneous strain. Phase transitions in $DyVO_4$ [20,21], TeO_2 [22], $BiVO_4$ [23], and NdP_5O_{14} [24] verify this property. As shown in Table I application of electric fields to the ferroelastic phases of the four compounds induce a ηP^2 coupling for E_{xy} fields, with the emergence of FI or WF phases, or only a $\eta^2 P^2$ coupling for fields along z, giving rise to a FE phase. AFE dielectric anomalies have been reported at the transitions in $DyVO_4$ [20,21] and TeO_2 [22]. ηP^3 couplings are allowed at *ferroelastoelectric* transitions [25] where the AFE order parameter has the symmetry of a third-rank piezoelectric tensor component. ηP^4 couplings are found in proper *ferrobielastic* transitions [25] where the order parameter has the symmetry of an elastic stiffness.

IV. DISCUSSION

Our extended investigation of structural transitions to nonpolar phases shows that although conditions 1 and 2 are satisfied in a large number of materials, the emergence of a FE phase above a coercive field may not always occur because of the large energy difference between the low-field FI and high-field FE phases. This is due, in particular, to the additional strains possibly required for stabilizing the FE phase. For example, at the AFE transition in $NH_4H_2PO_4$, a double hysteresis loop could not be observed [16], the onset of a FE phase implying an orthorhombic deformation of its monoclinic or triclinic FI phase. Therefore, antiferroelectrics presenting all the dielectric features currently assumed for PA–AFE transitions should not constitute a widespread class of materials, as compared to ferroelectrics. This is in contrast to antiferromagnets which form the largest class of magnetically ordered materials. However, our proposed definition of PA–AFE transitions, given in Sec. II, does not imply the stabilization of a FE phase under applied field or a double hysteresis loop, and extends the current characterization of antiferroelectrics to the larger class of materials in which a polar (FI or WF) field-induced phase emerges from a nonpolar phase.

The analogy between antiferromagnets and antiferroelectrics is usually invoked because both antiferromagnetic and AFE structures display antiparallel arrays of spins or dipoles and because ferromagnetic or FE phases emerge above coercive fields. Our work underlines a deeper analogy consisting of the common microscopic nature of the symmetry-breaking order parameter in the two classes of materials: the emergence of a discrete array of local dipolar sites, which constitutes in our approach the microscopic symmetry-breaking mechanism for the formation of an AFE phase, is the structural analog of the continuous microscopic spin-density waves which are the symmetry-breaking order parameters at antiferromagnetic transitions. It can be questioned if the analogy extends at the level of the interactions between dipoles, i.e., if there exists a physical criterion characterizing AFE interactions, similar to the negative sign of the exchange interaction typifying antiferromagnets. In this respect it can be noted that all experimental examples of AFE transitions show a decrease of the dielectric permittivity, corresponding to a positive sign of the coupling coefficient δ between η and P. Such repulsive coupling is necessary for compensating the attractive (negative) interactions existing between antiparallel dipoles [26] and results from the different types of repulsive forces [27] between permanent and induced dipoles. By contrast, the dielectric permittivity at improper ferroelectric transitions undergoes an upward discontinuity [28] reflecting the attractive coupling between η and P required for compensating the repulsive interactions between parallel dipoles. Although such considerations need to be substantiated by a detailed theoretical analysis they suggest that the decrease of the dielectric permittivity at a structural transition to a nonferroelectric phase denotes the presence of AFE interactions, in the same way that the shape of its magnetic susceptibility typifies an antiferromagnetic ordering.

The essential difference, noted in the Introduction of this article, between the time-reversal symmetry involved in magnetic transitions and the localized symmetries characterizing structural transitions, does not preclude a formal analogy between the theoretical approaches to magnetic and structural transitions, and this analogy can be used for deducing the still unknown fundamental properties of antiferroelectrics from the well established properties of antiferromagnets. However, one should keep in mind that although spin densities are localized, electric dipole densities localized at polarizable sites represent only a conceptual image which has been used for establishing the dielectric properties of polarized insulators.

In the case of AFE transitions this image can be specified in two different ways depending on the symmetry breaking mechanism occurring at the transition. If the transition induces a breaking of the translational periodicity associated with a wave vector $k \neq 0$, the AFE structure can be considered as formed by an alternation of unit cells having antiparallel local polarizations. For transitions without modification of the crystal unit cell ($k = 0$) one can separate in each unit cell two regions corresponding to antiparallel polarizations. In both cases the dipoles are assumed to be located at sites consistent with the symmetry operations of the AFE structures and represent the polarization of the entire surrounding volumes (unit cell or region of a unit cell).

The relation of the AFE order parameter η with the local distribution of dipoles can correspond to two different transition mechanisms, similar to the different mechanisms characterizing "proper" and "improper" ferroelectric transitions [28,29]. For proper AFE transitions η can be directly expressed in terms of the local dipole distribution either in a continuous formalism, as a polarization wave amplitude, or in a discrete formalism, as a linear combination $\Sigma(\vec{p}_i - \vec{p}_j)$ of local dipoles belonging to antiparallel arrays of emerging polar sites. For improper AFE transitions η represents a structural (displacive or ordering) mechanism which typifies the lowering of symmetry at the transition, the emergence of an antiparallel polarization wave amplitude being an induced secondary effect of the preceding primary mechanism.

V. SUMMARY AND CONCLUSION

In summary, AFE phase transitions have been shown to occur under combined local and macroscopic symmetry conditions, which provide a symmetry based definition of this class of structural transitions. A Landau theoretical description of their dielectric properties has been given by taking into account the electric-field induced couplings existing between the AFE and polarization order parameters. This description leads to properties of AFE materials differing essentially from the properties deduced from Kittel's model of antiferroelectrics [8]: the FE phase is absent from the phase diagram at zero field, its emergence as a purely field induced effect being conditioned by symmetry requirements. Furthermore, the AFE order parameter η may represent a structural mechanism inducing indirectly the antiparallel dipole lattices (improper antiferroelectricity), or can be expressed directly in terms of antiparallel dipoles (proper antiferroelectricity) as assumed by Kittel.

ACKNOWLEDGMENTS

The authors are grateful to B. Mettout for very helpful discussions and J. Kreisel for suggesting this work. Work supported by the National Research Fund, Luxembourg (FNR/P12/4853155/Kreisel).

[1] R. E. Birss, *Symmetry and Magnetism* (North-Holland, Amsterdam, 1966).
[2] K. M. Rabe, in *Functional Metal Oxides: New Science and Novel Applications*, edited by S. Ogale and V. Venkateshan (Wiley, New York, 2013).
[3] A. K. Tagantsev, K. Vaideeswaran, S. B. Vakhrushev, A. V. Filimonov, R. G. Burkovsky, A. Shaganov, D. Andronikova, A. I. Rudskoy, A. Q. R. Baron, H. Uchiyama, D. Chernyshov, A. Bosak, Z. Ujma, K. Roleder, A. Majchrowski, J.-H. Ko, and N. Setter, Nat. Commun. **4**, 2229 (2013).
[4] J. Hlinka, T. Ostapchuk, E. Buixaderas, C. Kadlec, P. Kuzel, I. Gregora, J. Kroupa, M. Savinov, A. Klic, J. Drahokoupil, I. Etxebarria, and J. Dec, Phys. Rev. Lett. **112**, 197601 (2014).
[5] J. F. Scott, Rev. Mod. Phys. **46**, 83 (1974).
[6] J. Roos, R. Kind, and J. Petzelt, Z. Phys. B **24**, 99 (1976).
[7] A. P. Levanyuk and D. G. Sannikov, Sov. Phys. JETP **28**, 134 (1969).
[8] C. Kittel, Phys. Rev. **82**, 729 (1951).
[9] K. Okada, Phys. Rev. Lett. **15**, 252 (1965).
[10] H. T. Stokes and D. M. Hatch, Phys. Rev. B **30**, 3845 (1984).
[11] S. Teslic and T. Egami, Acta Crystallogr., B **54**, 750 (1998).
[12] Y. Makita, J. Phys. Soc. Jpn. **20**, 1567 (1965).
[13] K. Gesi, J. Phys. Soc. Jpn. **33**, 561 (1972).
[14] J. Ortiz-Lopez and F. Luty, Phys. Rev. B **37**, 5452 (1988).
[15] W. P. Mason and B. T. Matthias, Phys. Rev. **88**, 477 (1952).
[16] W. Känzig, *Ferroelectrics and Antiferroelectrics* (Academic Press, New York, 1957).
[17] J. Feder, Ferroelectrics **12**, 71 (1976).
[18] W. J. Merz, Phys. Rev. **91**, 513 (1953).
[19] J.-C. Tolédano and P. Tolédano, Phys. Rev. B **21**, 1139 (1980).
[20] H. Unoki and T. Sakudo, Phys. Rev. Lett. **38**, 137 (1977).
[21] K. Kishimoto, T. Ishikura, H. Nakamura, Y. Wakabayashi, and T. Kimura, Phys. Rev. B **82**, 012103 (2010).
[22] P. S. Peercy and I. J. Fritz, Phys. Rev. Lett. **32**, 466 (1974).
[23] J. Bierlein and A. Sleight, Solid State Commun. **16**, 69 (1975).
[24] H. Schulz, K. H. Thiemann, and J. Fenner, Mater. Res. Bull. **9**, 1525 (1974).
[25] P. Tolédano and J.-C. Tolédano, Phys. Rev. B **16**, 386 (1977).
[26] H. Margenau and N. Kestner, *Theory of Intermolecular Forces* (Pergamon Press, New York, 1969).
[27] F. London, Trans. Faraday Soc. **33**, 8b (1937).
[28] A. P. Levanyuk and D. G. Sannikov, Usp. Fiz. Nauk **112**, 561 (1974).
[29] P. Tolédano and J.-C. Tolédano, Phys. Rev. B **14**, 3097 (1976).
[30] T. Omura, C. Moriyoshi, K. Itoh, S. Ikeda, and I. Fukazawa, Ferroelectrics **270**, 375 (2002).